An Investigation of the Electronic Properties of Cadmium Zinc Telluride Surfaces using Pulsed Laser Microwave Cavity Perturbation

Gary Tepper [a], Royal Kessick [a] and Csaba Szeles [b]

[a] Department of Chemical Engineering, Virginia Commonwealth University, Richmond, VA 23116

[b] eV Products, Saxonburg, PA 16056

ABSTRACT

The spectroscopic performance of cadmium zinc telluride (CZT) room temperature radiation detectors is currently limited by both bulk and surface imperfections introduced during the growth, harvesting and fabrication of these devices. Bulk imperfections including impurities, vacancies, interstitials, grain boundaries and dislocations have been relatively well studied and are known to trap charge and reduce detector performance. However, the effect of specific traps on the electronic decay process has been difficult to quantify. Surface imperfections including mechanical damage or adsorbed chemical species are also known to trap charge or increase leakage current, but it has proven difficult to characterize the electronic properties of CZT surfaces prior to electrode deposition. Here it is shown that the pulsed laser microwave cavity perturbation method can provide important information on the electronic decay process both in the bulk and at the surface of high pressure Bridgman CZT crystals. Electronic decay time was measured as a function of temperature and surface conditions. It is shown that the electronic decay process in bulk CZT is consistent with a single deep hole trap at an energy between 600meV and 700meV. The effect of surface quality was resolved by analyzing distinct features in the photoconductivity decay curves. Atomic force microscopy was used to characterize the surface roughness. Rough or damaged surfaces exhibited persistent photoconductivity, which could be eliminated by etching with a Bromine Methanol solution.

Keywords: Microwave Cavity Perturbation, Carrier Decay Time

1. INTRODUCTION

To obtain spectroscopic information on gamma-rays using $Cd_{1-x}Zn_xTe$ (x~0.1) (CZT) detectors, the charge carriers generated by the radiation must be transported from the bulk of the crystals to the electrodes on the surface and converted into a measurable signal. This process requires uniform, high-resistivity material exhibiting efficient charge transport. Bulk compensation mechanisms in CZT have been widely studied and high-resistivity (~10^{10} Ω-cm) CZT can now be grown through the careful introduction of complementary material defects or impurities that pin the Fermi level near the middle of the energy gap. The increase in the electrical resistivity of the material through compensation results in lower leakage currents and the ability to apply relatively large electric fields to the CZT detector devices. However, charge transport is still limited by trapping, both in the bulk and at the surface and the material yield, uniformity and maximum size of CZT spectrometers remains limited. Charge trapping within the bulk of the material has been studied using a number of techniques [1-3]. However, it has been difficult to study charge trapping and recombination effects on CZT surfaces because of the need to apply electrodes, which can influence the charge transport process. In this paper we present a study of electronic decay in CZT both in the bulk and at the surface using a contactless pulsed laser microwave cavity perturbation method. A detailed balance calculation is used to fit the experimental data and it is shown that the electronic decay process in detector grade CZT is consistent with a single deep recombination center with energy between 600meV and 700meV.

Photo generation of charge carriers in CZT is used to produce an associated increase in the material conductivity. Upon removal of the optical excitation, the conductivity returns to an equilibrium value (photoconductive decay) at a rate dependent on a variety of parameters including the availability and properties of the electron and hole traps within the material or at the surface. Various terms including carrier lifetime, trapping time, detrapping time and recombination time have been used to describe electronic decay in semiconductors. However, it is usually difficult to assign the decay process to one particular mechanism. Therefore, in the present work, a characteristic decay time (τ_e) will be used to describe the time constant associated with the electronic decay process and it should be understood that this parameter is influenced by a synergism of trapping and detrapping mechanisms.

In the initial stage of CZT detector fabrication, the crystal is mechanically cut from the source material. The cutting process introduces a surface damage layer that must be removed through a combination of mechanical polishing and chemical etching before electrodes are applied to the material. The surface condition is typically checked using profilometry or microscopy, which only provides surface topographical information and does not provide any information on the electrically active surface or near surface defects. In this manuscript, the electronic behavior of the crystal at various stages of surface preparation is investigated and the decay time is determined as a function of temperature. From these measurements, the contribution that surface effects play on electronic behavior of CZT detector devices is evaluated.

2. EXPERIMENTAL

The experimental apparatus has been described in detail in a previous publication and will only briefly be reviewed here [4]. Figure 1 is a schematic diagram illustrating the basic experimental configuration. A tunable solid-state YIG oscillator provides the microwave energy with a frequency range of 4 – 8 GHz and a maximum power output of 100mW. The microwave energy is directed through a waveguide and enters through an adjustable aperture into a TM_{010} cylindrical resonant cavity containing the semiconductor sample. The resonant frequency of the cavity is determined by its size and by the dielectric constant of the sample material and was approximately 6 GHz for the experiments reported here. The TM_{010} resonant mode provides a maximum electric field at the center of the cavity and the electric field magnitude can be estimated by balancing the cavity input power with the cavity loss under equilibrium conditions. A rigorous calculation of the electric field magnitude within the sample is complicated by factors including the sample geometry. Nevertheless, we qualitatively estimate that the electric field magnitude at the sample location is on the order of 100 V/cm.

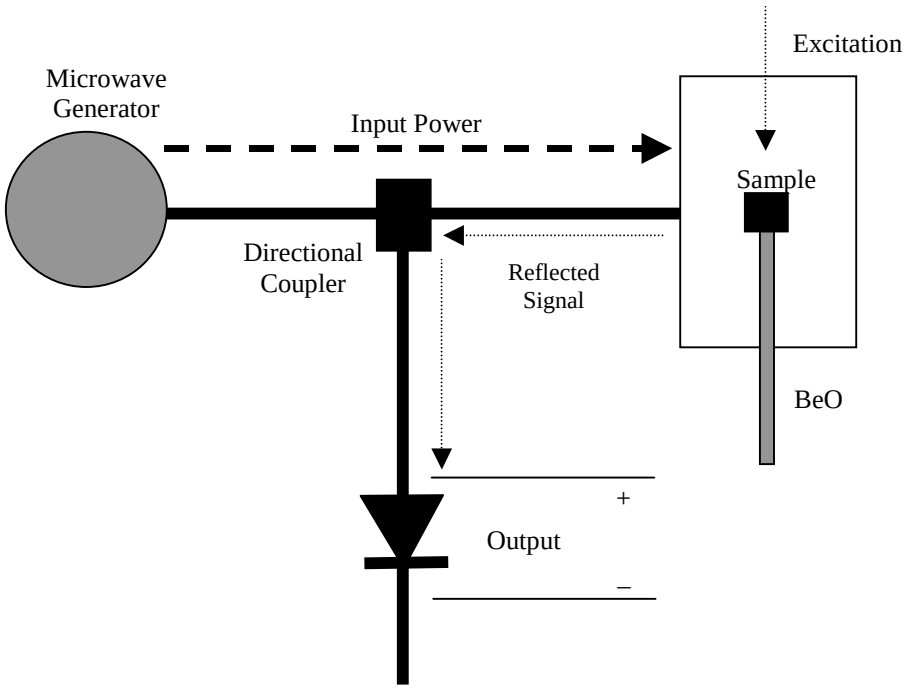

Figure 1: Schematic diagram of experimental apparatus

The change in the quality factor (Q) of the microwave cavity upon photo-excitation of the semiconductor sample is the basis for the technique. The photo-excitation in these experiments was provided by a pulsed Nd:YAG laser with a wavelength of 1064 nm and a pulse duration of approximately 7 ns. It should be noted that the laser photon energy is insufficient to directly excite carriers across the band gap in CZT. Therefore, the photo-generation process is restricted to other mechanisms including trap ionization, phonon assisted or multiphoton excitation. The laser energy could be continuously adjusted to a maximum of 90 mJ. A 1 mm diameter circular aperture was machined into the side of the cavity for the photo-illumination. The semiconductor sample was inserted axially into the center of the cavity using a cylindrical BeO rod. BeO is an electrical insulator and, therefore, creates negligible load to the cavity compared to the CZT sample. However, the thermal conductivity of BeO is quite high and the sample could therefore be cooled to approximately 89K by placing the external end of the rod into a liquid nitrogen reservoir without the need to introduce coolant directly into the cavity. Condensation inside the cavity was avoided by keeping the cavity under a constant positive pressure of inert gas.

After the photoexcitation is removed, the conductivity of the sample and quality factor of the cavity return to the equilibrium values at a rate dependent on the electronic decay process in the sample. The change in the quality factor is detected through the corresponding change in the reflected microwave power. Thus, the decay time is determined by observing the time dependence of the reflected microwave power immediately following the sample excitation.

The CZT samples studied in this work were grown at eV PRODUCTS using a high pressure Bridgman method from high purity starting materials in graphite crucibles [5,6]. The $5\times5\times2$ mm^3 and $10\times10\times2$ mm^3 samples were cut from the large-grain polycrystalline ingots using an ID and dicing saw. The samples were selected from various ingots to cover the electron lifetime range between 2×10^{-7} s to 3×10^{-6} s. The lifetimes were extracted from mobility-lifetime measurements by fitting the Hecht relationship to the voltage dependence of the 59.5 keV photopeak peak position in parallel plate detector devices fabricated from the

samples. Pt electrodes were deposited on the surface of the samples by sputtering for these initial lifetime measurements. The electrodes were then removed in order to characterize the electronic decay using the contactless microwave technique.

3. RESULTS AND DISCUSSION

Figure 2 is a plot of the normalized reflected microwave power verses time for the pulsed illumination of a CZT sample at various temperatures ranging from 89K to 250K. The surface of the crystal had been polished and etched to remove the damage layer introduced during cutting in preparation for electrode deposition. The reflected microwave signal intensity is a measure of the free charge carrier density as a function of time and the signal decay can be described mathematically by a series of exponential functions with independent time constants. In general, the decay process is governed by a synergism of trapping, and detrapping mechanisms, which depend on temperature. Characteristic decay times were calculated by fitting a region of the decay profiles from 85% to 60% of the peak to a single exponential and are plotted as a function of temperature in figure 3. As can be seen in figure 3, the carrier lifetimes are longest at low temperature, decrease rather rapidly with temperature until about 160K and then level off. Also shown in figure 3 are dashed lines that are the result of a detailed balance calculation modeling the electronic decay process in CZT as a function of temperature. The model is described in the following section.

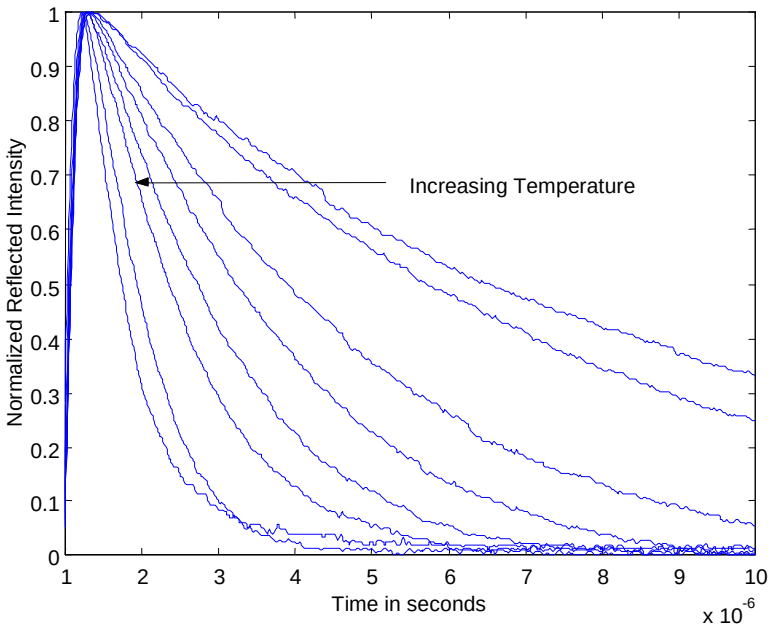

Figure 2: Normalized reflected signal intensity versus time from 250K to 89K.

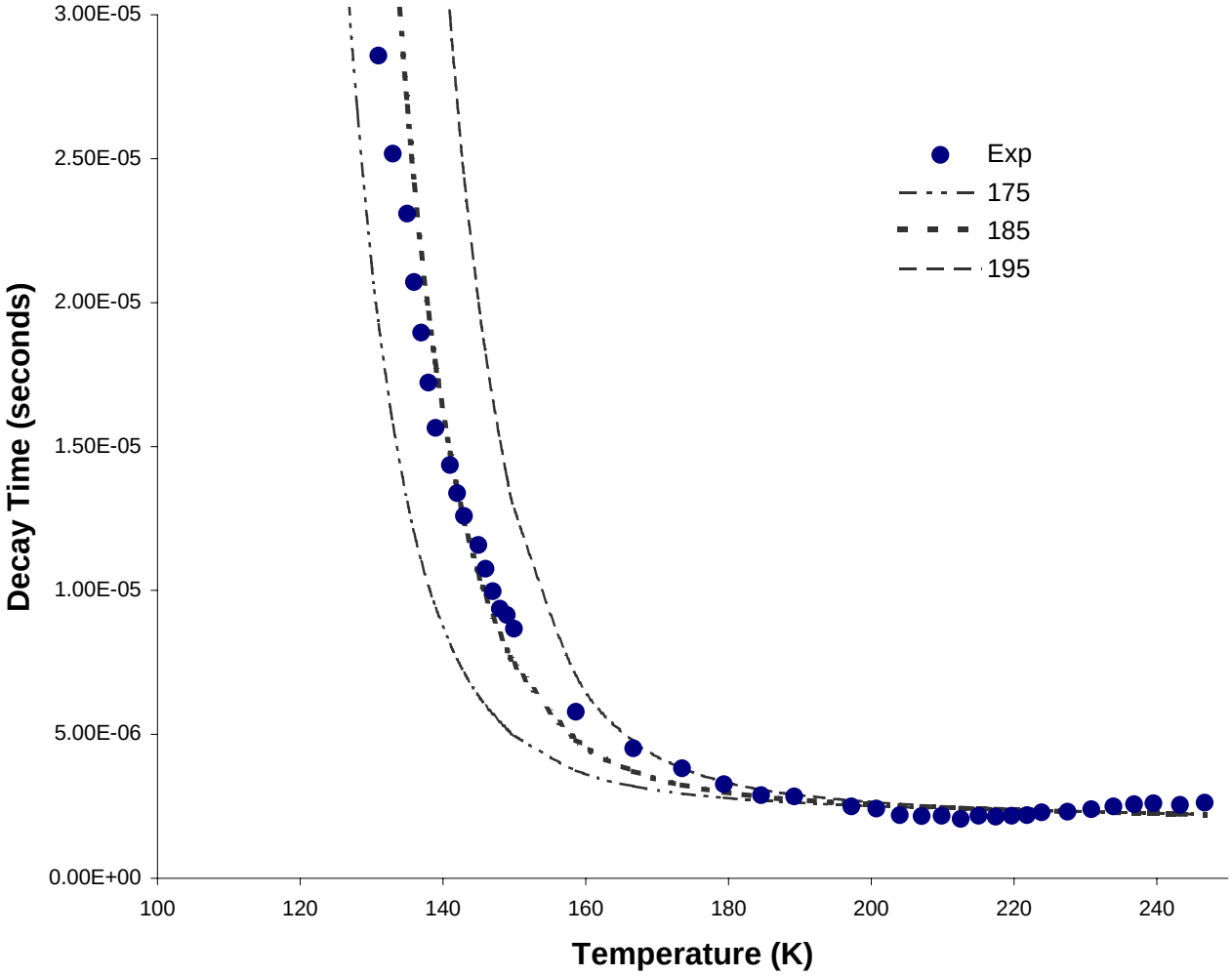

Figure 3: Plot of decay time versus temperature. The dots are the experimental data. The dashed lines are the results of a trapping model.

3.1 Trapping Model:

The photogenerated electrons and holes are separated through the application of an electric field and the dominant recombination process is therefore assumed to be indirect transitions via localized energy states (traps or recombination centers) in the band gap. After the pulsed photoexcitation, the sample conductivity returns to an equilibrium condition at a rate that can be estimated using the principle of detailed balance. That is, in order to restore equilibrium, the electron and hole trapping rates will exceed the detrapping rates. For simplicity we will assume that, initially following the excitation, the rate of change in the free electron and hole concentrations are equal. That is:

$$dn/dt = dp/dt \tag{1}$$

This condition is normally satisfied when the recombination process is rate limited by the minority carrier decay. For example, in an n-type semiconductor under low injection conditions, the free electron concentration far exceeds the free hole concentration. Consider the case of a recombination center (trap) at an energy level E_t that is neutral when unoccupied. When a hole is trapped, the charge-state of the neutral trap becomes positive and the capture cross section for the majority carriers increases significantly. Thus, hole capture is the rate-limiting step and equation 1 is valid. Equation 1 can be rewritten in the following form:

$$T_e - D_e = T_h - D_h, \tag{2}$$

where T_e and T_h are the electron and hole trapping rates and D_e and D_h are the electron and hole detrapping rates respectively. The trapping and detrapping rates for electrons and holes in equation 2 can be expressed in terms of the material parameters. For electrons, the concentration of unoccupied centers is given by $N_t(1-F)$, where N_t is the trap concentration and F is the Fermi distribution function given by

$$F = 1/\{1 + \exp[(E_t - E_F)/kT]\}, \tag{3}$$

where E_F is the Fermi energy. The electron trapping rate is therefore

$$T_e = v_{th}\sigma_e n N_t(1-F), \tag{4}$$

where v_{th} is the electron thermal velocity $\{v_{th} = (3kT/m_e)^{1/2}\}$, σ_e is the trap capture cross section and n is the concentration of free electrons at thermal equilibrium and is given by

$$n = n_i \exp\{(E_F - E_i)/kT\}, \tag{5}$$

where n_i is the intrinsic carrier concentration and E_i is the intrinsic Fermi energy (the mid gap energy). The electron detrapping rate is given by

$$D_e = v_{th}\sigma_e n_i N_t F \exp\{(E_t - E_i)/kT\}. \tag{6}$$

From this equation it can be seen that the detrapping rate increases as the trap energy approaches the conduction band energy. Similarly, the hole trapping rate is given by

$$T_h = v_{th}\sigma_h p N_t F, \tag{7}$$

where v_{th} is now the thermal velocity of holes, σ_h is the hole capture cross section and p is the hole concentration. Finally the hole detrapping rate is given by

$$D_h = v_{th}\sigma_h n_i N_t(1-F) \exp\{(E_i - E_t)/kT\}. \tag{8}$$

Inserting equations 4, 6, 7 and 8 into equation 2 we can solve for the net recombination rate as $R = T_e - D_e$. If we further assume low injection conditions for an n-type semiconductor (i.e. $n_n >> p_n$) and also assume that the electron and hole capture cross sections are equal ($\sigma_e = \sigma_h$) it follows that

$$R = (p_n - p_{no})/\tau_e, \tag{9}$$

where p_n and p_{no} are the hole concentrations under photoexcitation and thermal equilibrium respectively and τ_e is the electronic decay time given by

$$\tau_e = \tau_o[1 + (2n_i/n_{no})\cosh\{(E_t-E_i)/kT\}], \tag{10}$$

where

$$\tau_o = 1/v_{th}\sigma N_t \tag{11}$$

and n_{no} is the free electron concentration under thermal equilibrium. The CZT samples used in this investigation have a measured resistivity on the order of 10^{10} Ω–cm, so that n_{no} is approximately 10^6 carriers/cm^3. Due to the relatively large band gap in CZT, the intrinsic carrier concentration (n_i) is very low. If we assume $n_i \sim 1/cm^3$, equation 10 becomes

$$\tau_e = \tau_o[1 + (10^{-6})\cosh\{(E_t-E_i)/kT\}]. \tag{12}$$

The first term on the right hand side of equation 12 is the minimum trapping or decay time, given in equation 11. The second term takes into account the dependence of the decay time on the trap energy E_t. For deep traps ($E_t - E_i < 10kT$), the second term is small and the decay time is essentially equal to τ_o. For $E_t - E_i > 10kT$, the second term increases exponentially and quickly dominates. Equation 10 is plotted as a function of temperature in figure 3 for three trap energies and using a value of 3.5μs for τ_o. As can be seen in the figure, the model is very sensitive to the trap energy and matches the experimental data very well for $E_t - E_i = 185meV$. The excellent agreement between the model and the experimental data was somewhat surprising because the model assumes that the electronic decay process is governed by a single recombination center at energy between 600meV and 700meV from the band edge. Previous investigations of detector grade CZT have identified several electron and hole traps at various energies throughout the band gap. However, our results suggest that one particular trap dominates the electronic decay in CZT. Recent investigations of the trap energies in detector grade CZT have reported a deep hole trap at an energy that is consistent with our results [1,2].

3.2 Surface Effects

It is well known that the surface region can be a source of a large number of localized energy states, which can act as traps or recombination centers. Figure 4 is a plot of reflected microwave intensity versus time at various temperatures for an as-cut CZT sample. The data in figure 4 was obtained under identical operating conditions as the data in figure 2. The decay profiles are very different for the damaged sample in comparison to the undamaged sample of figure 2. For all temperatures, two distinct regions can be identified. Initially (for about the first 2 microseconds) the decay is relatively rapid. Then there is a transition region followed by a region of slow decay. In fact, we have found that in some of the damaged samples, the conductivity does not return to equilibrium even after several milliseconds. We therefore assume that this "persistent photoconductivity" is associated with surface trap states introduced by the mechanical damage. The electronic decay in the damaged samples can not be described by a single decay time and a more comprehensive model will be necessary in order to relate the decay profiles to trap energies. Nevertheless, we can qualitatively relate surface quality and damage recovery to certain specific features in the electonic decay profile.

A Br/MeOH solution was used to etch away the surface damage in an as-cut crystal and decay curves were obtained between each etch. Figure 5 is a plot of reflected microwave power versus time for the pulsed

illumination of a CZT sample at 89K as a function of surface quality (etch time). As stated above, the heavily damaged surface results in a decay profile with two distinct regions. Initially the decay is relatively fast and then levels off to a state of persistent photoconductivity characterized by a lifetime in the millisecond range. As the surface quality is improved by etching with the Br/MeOH solution, the initial decay time increases and the persistent photoconductivity eventually disappears. As stated before, we believe that the damaged surface region has a multitude of charge traps that result in a decrease in the low temperature lifetime with respect to the etched surface. The persistent photoconductivity observed in figure 4 may be the result of very slow detrapping from a new shallow trap state associated with the damaged region. As the damaged region is removed the decay curves return to a shape similar to the high quality samples of figure 2.

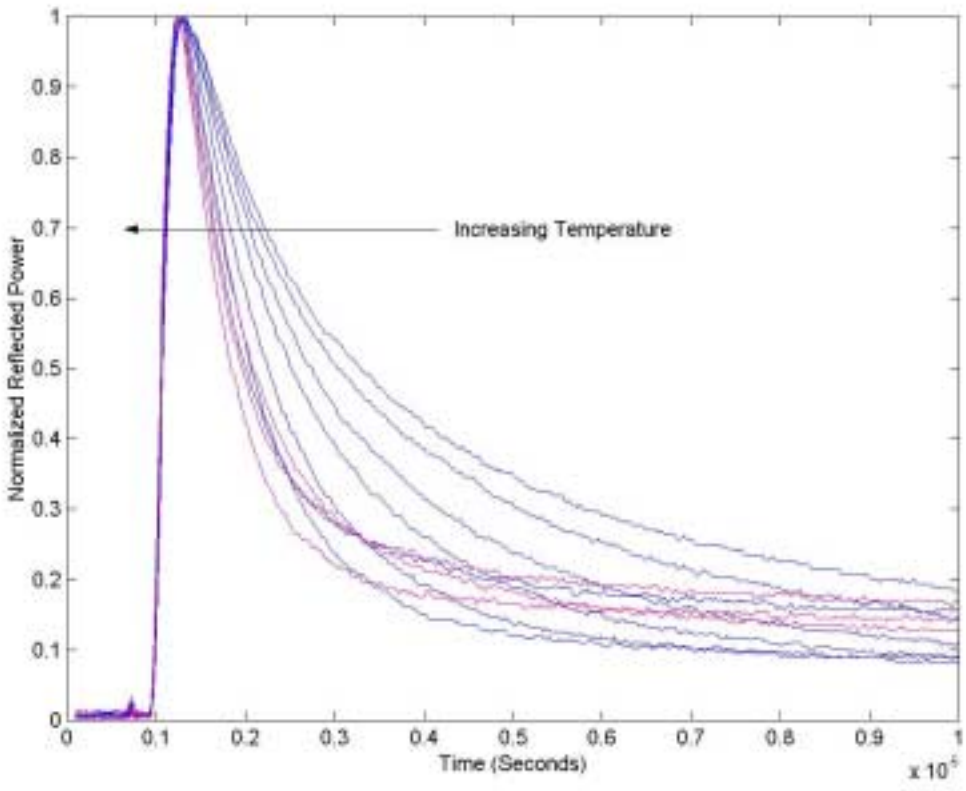

Figure 4: Reflected microwave power versus time from 250K to 89K for an as-cut CZT sample.

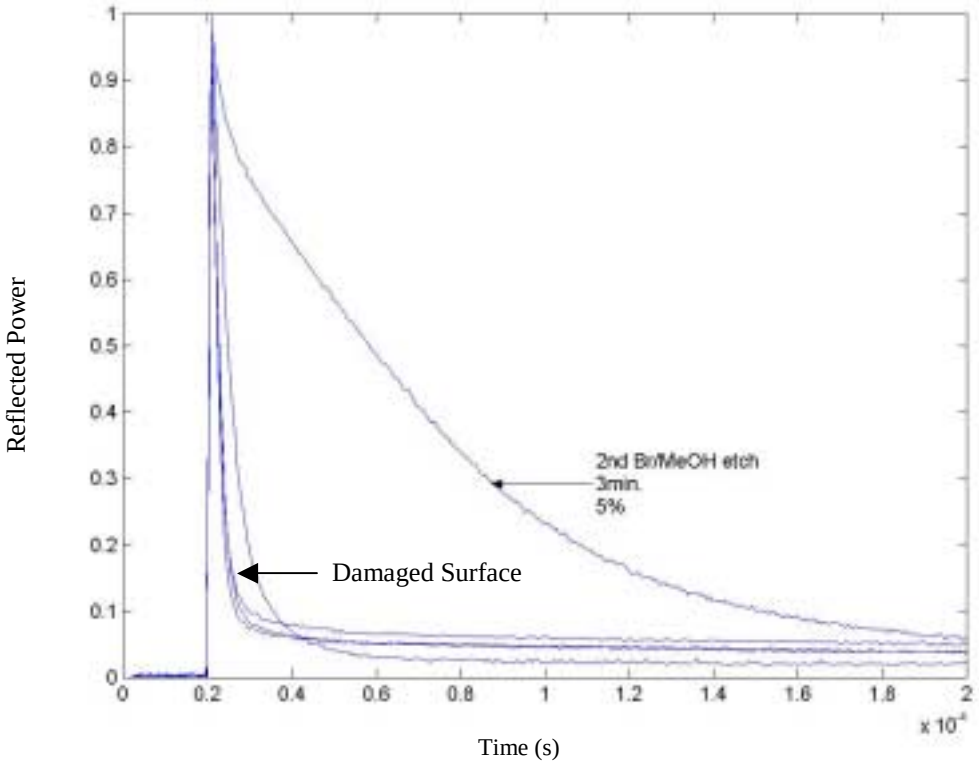

Figure 5: Reflected microwave power versus time showing damage recovery during etching. Sample temperature: 89K

a b

Figure 6: (a) as-cut surface, 7-8μm roughness, (b) etched surface ~.6μm roughness. 10X magnification with IR microscope

The damaged and etched crystal surfaces were also studied using optical microscopy and are shown in figure 6. The black damaged layer from the initial surface has been almost completely removed by the etch. However, the etched surface still exhibits cluster-like formations, which we interpret as the remnants of the surface damage. The mean surface roughness values for the as-cut and etched surfaces are 7-8 μm to approximately 0.6μm, respectively. Due to the high level of roughness on the initial sample a linear profilometer was used to quantify the roughness. For the etched surface AFM was used to characterize the surface roughness.

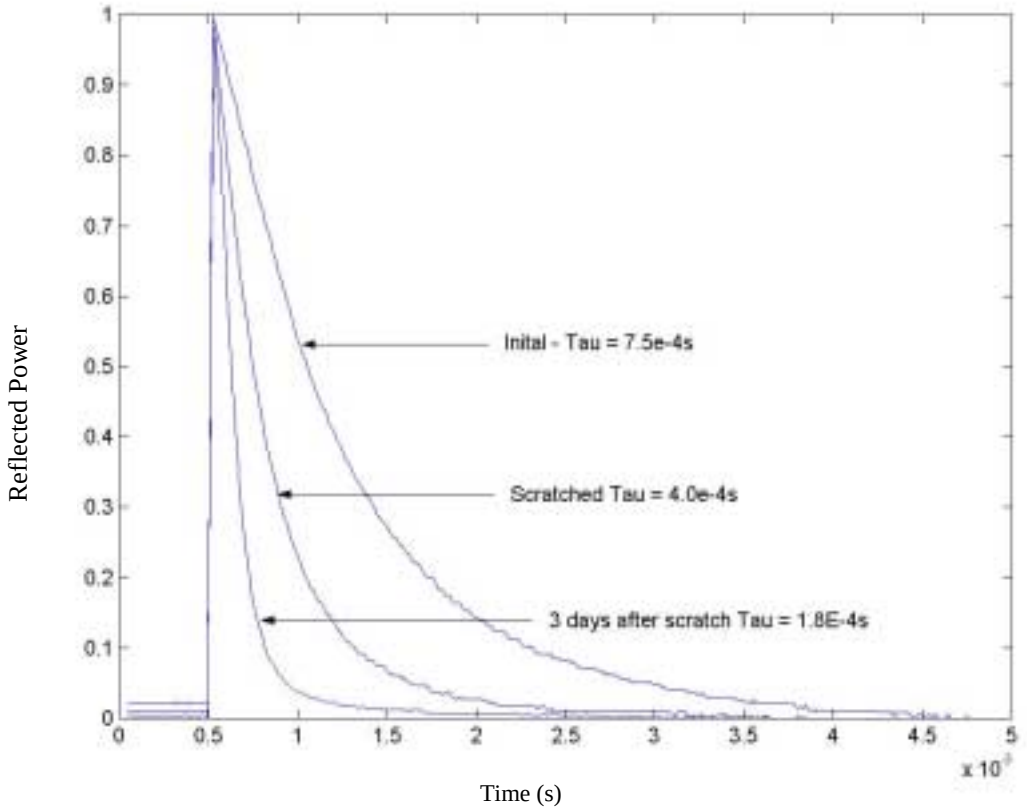

Figure 7: Reflected microwave intensity versus time illustrating introduction of surface damage and subsequent oxidation (sample temperature = 89K).

As a final test we examined the effects of reintroducing surface damage on an etched sample. Figure 7 is a plot of reflected microwave power versus time for a CZT sample at 89K at three different surface conditions. Initially the surface quality was high and the effective carrier lifetime at 89K was very long as was expected. Next, the surface was scratched using fine emery cloth and the effective carrier lifetime immediately decreased by about a factor of 2. Finally after three days we re-tested the scratched surface and found that the lifetime had decreased by another factor of two. This suggests that the initial decrease in decay time is due to the introduction of additional charge traps at the surface. The subsequent decrease in carrier lifetime may be due to surface oxidation. However, CZT surfaces are known to oxidize very rapidly and were expected to have reached a steady state condition immediately after the introduction of damage. A recent investigation has shown that dislocations in CZT are mobile even at room temperature[7]. Therefore, an alternate explanation for the time dependent decrease in the decay time due to surface damage is the migration of dislocations from the surface into the bulk. We also point out that no persistent photoconductivity was observed in the data of figure 7 and hypothesize that the damage introduced by the emery cloth is insufficient to produce the traps associated with the persistent photoconductivity observed in figure 4.

4. CONCLUSIONS

An investigation of the electronic decay in detector grade cadmium zinc telluride as a function of temperature and surface quality has been investigated using a contactless pulsed laser microwave cavity perturbation technique. The results indicate that the electronic decay process in the bulk is dominated by a single deep hole trap at an energy of between 600meV and 700meV above the valence band. The electronic decay process at the surface is more complicated and is a strong function of surface quality. The results show that the quality of the CZT surface strongly influences the electronic decay time, particularly at low temperature. We propose that the surface damage introduces a multitude of charge traps at various energies. These traps can be removed by a chemical etch and the damage recovery process can be monitored using the contactless microwave technique. The contactless microwave technique described here, therefore, provides a convenient method of analyzing the electronic behavior of CZT both at the surface and in the bulk without the need to make electrical contacts.

ACKNOWLEDGEMENTS

Funding for this work was provided in part by the Ballistic Missile Defense Organization and the Jeffress Memorial Trust Fund.

REFERENCES:

1. E.Y. Lee, R.B. James, R.W. Olsen, and H. Hermon, "Compensation and Trapping in CdZnTe Radiation Detectors Studied by Thermoelectric Emission Spectroscopy, Thermally Stimulated Conductivity, and Current-Voltage Measurements", *Journal of Electronic Materials*, Vol. **28**, No. 6, 766 (1999)
2. A. Castaldini, A. Cavallini, B. Fraboni, P. Fernandez, and J. Piqueras, "Deep Energy Levels in CdTe and CdZnTe", *Journal of Applied Phyics*, Vol., **83**, No. 4, 2121 (1998)
3. T. Thio and J.W. Bennett, "Deep Donors in CdZnTe:Cl", *Physical Review B*, Vol. **54**, No. 3, 1754 (1996)
4. Royal Kessick, Gary Tepper**,** Ed Lee and Ralph James, "Thermally Stimulated Carrier Lifetime Measurements in Detector Grade Cadmium Zinc Telluride", *Journal of Applied Physics*, **87**, 2408 (2000)
5. Cs. Szeles and E.E. Eissler, "Current Issues of High-pressure Bridgman Growth of semi-insulating CdZnTe", *MRS Symposium Proceedings*, Vol. **487**, (MRS, Warrendale, 1998), p. 3.
6. Cs. Szeles and M.C. Driver, "Growth and properties of semi-insulating CdZnTe for radiation detector applications", *SPIE Proceedings Series*, Vol. **3446**, 2 (1998).
7. K.G. Lynn and Cs. Szeles, Private communication